Computer Simulation Study of tert-Butyl Alcohol. 1. Structure in the Pure Liquid

ARTICLE · SEPTEMBER 2000

CITATIONS
7

READS
23

1 AUTHOR:

Peter G Kusalik
The University of Calgary
114 PUBLICATIONS **3,979** CITATIONS

SEE PROFILE

Computer Simulation Study of *tert*-Butyl Alcohol. 1. Structure in the Pure Liquid

Peter G. Kusalik

Department of Chemistry, Dalhousie University, Halifax, Nova Scotia, Canada B3H 4J3

Alexander P. Lyubartsev, Dan L. Bergman, and Aatto Laaksonen*

Division of Physical Chemistry, Arrhenius Laboratory, Stockholm University, S-10691 Stockholm, Sweden

Received: May 23, 2000; In Final Form: July 6, 2000

MD simulations of neat liquid *tert*-butyl alcohol (TBA) are carried out. Two very different potential models have been constructed for TBA: a simple rigid three-site model and a fully flexible all-atom 15-site model, with the O−H stretching described with an anharmonic potential well. Pure liquid TBA is investigated to evaluate the two potential models and to study the liquid structure in more detail. An analysis based upon both radial distribution functions and spatial distribution functions is employed. Generally it is found that the 15-site model is superior, providing reasonable agreement with experimentally derived data, while the three-site model is only able to reproduce qualitatively the competitive hydrophobic and hydrophilic aspects of the intermolecular interactions. Overall the structures observed reflect a frustrated hydrogen-bonded system.

Introduction

Simple, monohydric alcohols are chemically and physically important as model molecules and solvents. Also, their aqueous solutions and mixtures possess many specific properties due to strongly nonideal behavior. The amphiphilic character of alcohols as solutes has been observed to affect both the structure of the surrounding water and to promote their own aggregation in aqueous solution.[1]

Computer simulations of associated liquids and solutions have played an important role in providing insight into the structural, thermodynamical and dynamical aspects of solvation.[2] No other method can give as much detailed microscopic information as molecular dynamics (MD) or Monte Carlo (MC) simulations, especially when coordinated with suitable experiments to ensure the reliability of the models used.[3] In the present work, we report MD simulations of *tert*-butyl alcohol (TBA) using two new intermolecular potential models to investigate the spatial liquid structure and hydrogen bonding in neat liquid TBA.

All the four isomers of butyl alcohol, *n*-butyl, iso-butyl, *sec*-butyl, and *tert*-butyl, are among the most important industrial organic chemical products.[4] It should also be noted that the *sec*-butyl alcohol exists as two stereoisomers (D and L), with slightly different physical properties than observed in the racemic (*d,l*) mixture.[4] Most physical properties of these monohydric alcohols either increase or decrease monotonically across the series *n*-, iso-, *sec*- and *tert*-, with one very distinct exception: the freezing points (in °C) are −89.3, −108, −114.7 and +25.66. Astonishingly, the *tert*-butyl isomer freezes at temperatures more than 100° degrees higher than the other alcohols in this series. Its effectively spherical form apparently makes it much easier to pack and H-bond in its crystal form than the three other isomers with their more flexible alkyl groups.

In the case of solubility in water, the *tert*-butyl alcohol differs from the others by being readily soluble in all proportions while the others are only sparsely soluble in water. Solutions of TBA in water show an anomalously large volume contraction, indicating that the bulky trimethyl groups must be more readily accommodated into the water structure. At the same time the hydrophobic surface of the alkyl group is believed to enhance the water structure around it due to hydrophobic effects.[1] In the successive paper, we report a detailed study of the hydration structure of TBA and its tendency to aggerate in water upon increasing the TBA concentration.[5]

A number of computer simulation studies have been reported on TBA, both in dilute aqueous solutions and as a pure liquid. Fornili and co-workers[6] calculated an optimized geometry for TBA and its interaction with water at the Hartree−Fock 6-31G-(p,d) level. They then used this potential to perform MD simulations to investigate the hydration structure around TBA and compared it to that around trimethylamine-*N*-oxide, $(CH_3)_3$ NO. Only an infinitely dilute solution was studied. TBA was simulated as a pure liquid by Yonker et al., who followed the effects of pressure and temperature on the dynamics of TBA[7] in their combined NMR and MD work. A polarizable intermolecular potential function is constructed for TBA and a series of other simple alkanols and used in an MM/QM MC simulations by Gao and co-workers.[8] Bowron et al.[9,10] have used the method of empirical potential structural refinement as an aid to resolve their experimental structure factors into partial pair correlation functions. A few other similar compounds, with the bulky tri-methyl group, that have also been simulated are: *tert*-butyl chloride,[11,12] *tert*-butyl cyanide,[13] and *tert*-butylammonium chloride, $(CH_3)_3$ NHCl.[14]

In this paper we report MD simulation studies of two potential models, one an all-atom description and a second much simpler potential where the *tert*-butyl group is represented by a single interaction site. The structure in the pure liquids is examined and compared in detail with the aid of both radial and spatial distribution functions.

The outline of this paper is the following: after giving the details of the two potential models used and the computational

* Corresponding author. E-mail: aatto@tom.fos.su.se. Phone: +46 8 162372. Fax: +46 8 152187.

10.1021/jp001886w CCC: $19.00
Published on Web 09/20/2000

aspects in section II, we discuss our results for the structure of pure TBA in section III. Finally, our conclusions are given in section IV.

Computational Aspects

Molecular Models. We might expect the results of the simulations of TBA to be sensitive to the details of the potential models, where a reasonably delicate balance between steric and packing ("hydrophobic") effects, and hydrogen bonding ("hydrophilic") types of interactions should be present. Hence it is important that the choice of model should be made carefully. For example, an all-atom model should contain all the various internal modes of motion, including the degrees of freedom resulting from the four different internal rotations. A comparable water model should be chosen for balanced cross-interactions between the two molecules. Two obvious first choices for the potential models for TBA are a fully atomic 15-site model and a united atom, six-site model where the three methyl groups (with a total of 12 atoms) are collapsed into three interaction sites. As we will see, even the united atom six-site model can be simplified further by representing the entire *tert*-butyl group as a single interaction site.

An Overview of Previous Potential Models for TBA. The earlier computer simulation of TBA in a dilute water solution carried out by Nakanishi and co-workers[15] utilized an all-atom rigid model. They developed a TBA−water potential of the (12−6−1) type from TBA−water dimer energies, calculated at the limited Hartree−Fock (HF) STO-3G level of approximation, where two virtual charges were placed above the alcohol oxygen atom to mimic the lone pairs; no charge was put on the oxygen itself. For the water potential they employed the MCY model.[16] In subsequent work,[17] they simulated the same solution at a finite 3 mol% concentration with a new ab initio TBA−TBA potential. Again the HF STO-3G level was used to fit the energies to a (12−6−3−1) functional form. They did not report simulations of pure liquid TBA, however. Noto et al.[6] developed a similar all-atom model at the HF level using a double-ζ Gaussian basis set with polarization (DZP), corresponding to the 6-31G(d,p) notation. The geometry was first optimized at the same level of accuracy. The energy surface was fitted to a (10−4−2−1) potential and the atomic charges were taken from a Mulliken population analysis. Noto et al.[6] also used the MCY water model. Gao et al.[8] employed a pairwise additive component, consisting of the familiar Lennard-Jones and Coulombic form, and a nonadditive polarization term. The empirical parameters were optimized through a series of statistical Monte Carlo simulations.

It is straightforward to construct the OPLS model for TBA based on the work on alcohols by Jorgensen and co-workers.[18,19] This was done by Yonker et al.[7] in their examination of the temperature and pressure effects on the dynamics of TBA. However, they varied the Lennard-Jones parameters systematically to obtain a reasonable agreement with their NMR results. The OPLS model was used also by Bowron et al.[9] in their work to resolve the experimental partial structure of pure liquid TBA. In the OPLS model, the CH_n- groups are modeled as united atoms and the internal rotation of the $-C(CH_3)_3$ group is described with a four-term Fourier series.

In Table 1 we give the sets of fractional charges, gathered from the various studies mentioned above. Obviously a balanced set of charges on the hydroxyl groups is very important in describing the hydrogen bonding properties of TBA with themselves (and most importantly with the water molecules in the aqueous solutions). We can see, however, that the fractional charges differ quite significantly between the different models used in previous simulations.

TABLE 1: Fractional Charges Used in Various Potential Models for TBA

	Nakanishi et al.[a]	Yonker et al.[b]	Noto et al.	model I[c]
H (hydroxyl)	0.7175	0.435	0.3278	0.33
O (hydroxyl)		−0.700	−0.5723	−0.57
lp (hydroxyl)	−0.6765			
C (*tert*-butyl)	0.6355	0.265	0.3881	
com (*tert*-butyl)				0.24
C (methyl)			−0.3510	
H (methyl)			0.1010	

[a] The charge on the hydroxyl hydrogen is the same as the charge on the hydrogen in the MCY water model.[16] lp denotes the two lone pair positions above the oxygen. For more details, see ref 15. [b] These charges are given in the OPLS model.[18,19] [c] Our three-site model (for details, see the text). These charges are adapted from the work by Noto et al.

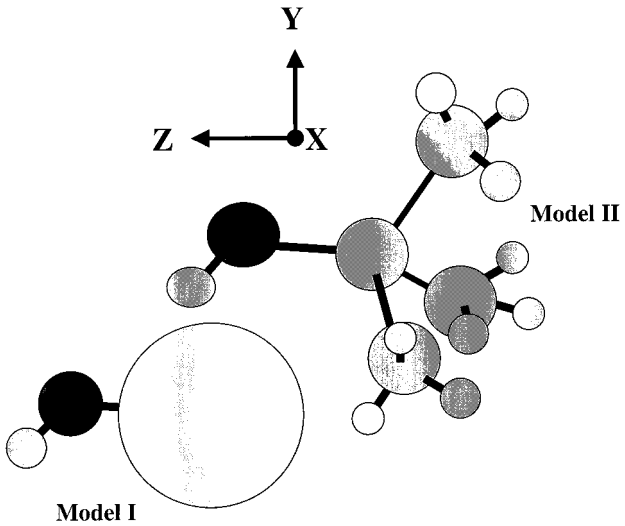

Figure 1. Molecular geometry for the two models for $(CH_3)_3COH$ used in the current work.

Potential Models Used in this Work. Since TBA can be considered as a simple model for both surfactants and some classes of biomolecules, one might expect the balance between hydrophobic and hydrophilic interactions to be rather important. Keeping this aspect in mind, we have constructed two very different potentials (force fields) for *tert*-butyl alcohol. We will simply refer to them as "model I" and "model II", respectively. One of our goals is to help identify the essential components of a TBA model.

Model I. This is a rigid three-site model, similar to that developed for methanol by Haughney et al.[20] (see Figure 1). Considering that TBA contains 15 atoms, this may immediately appear as a drastic simplification, but at the same time it considerably reduces the required computing time. The model has a single large Lennard-Jones sphere to mimic the $C(CH_3)_3-$ group; this is the simplest possible representation of this bulky hydrophobic group. Attached to this sphere is the hydroxyl group. This "double" united atom model is designed to eliminate, not only the degrees of freedom due to methyl group rotations, but also those due to the rotation of the whole trimethyl group itself. Potential parameters and the molecular geometries are given in Table 2. The Lennard-Jones parameter σ for the trimethyl group was estimated from the experimental radial distribution functions reported by Bowron et al.[9] The ϵ is about 10% larger compared to that for the united atom methyl model of methanol by Haughney et al.[20] The two bond lengths and the bond angle are taken from the geometry optimization

TABLE 2: Potential Parameters and Molecular Geometries for the Three-site Model (model I) of *tert*-butyl Alcohol and for SPC/E Water: tb Denotes the *tert*-butyl Group

	ϵ (kJ/mol)	σ (Å)	q (e)
$(CH_3)_3COH$[a]			
tb	0.8374	4.40	0.24
O	0.7327	3.083	−0.57
H	0.0	0.0	+0.33
H_2O[b]			
O	0.6506	3.1656	−0.8476
H	0.0	0.0	+0.4238

[a] R(O−H): 0.93 Å. R(tb−O): 1.836 Å. ∠tb−O−H: 111.2°. [b] R(O−H): 1.00 Å. ∠H−O−H: 109.47°.

TABLE 3: Nonbonded Potential Parameters and Molecular Geometries for the 15-site Model (model II) of *tert*-butyl Alcohol

	nonbonded interactions		
$(CH_3)_3COH$[a]	ϵ (kJ/mol)	σ (Å)	q (units of e)
O	0.67	3.00	−0.5723
C(*tert*-butyl)	0.1674	3.80	0.3885
C(methyl)	0.1674	3.80	−0.3510
H(methyl)	0.1674	2.40	0.1010
H(hydroxyl)	0.0	0.0	0.3278

[a] R(O−H): 0.9292 Å. $R(C_{tb}-O)$: 1.4164 Å. $\angle C_{tb}-O-H$: 111.28°. $R(C_{tb}-C_m)$: 1.524 Å. $R(C_m-H_m)$: 1.0887 Å. $\angle C_m-C_{tb}-C_m$: 108.0°. $\angle H_m-C_m-H_m$: 108.75°. Note, tb denotes *tert*-butyl and m methyl group

of Noto et al.[6] after locating the center-of-mass for the *tert*-butyl group. The atomic charges are essentially the same as those of Noto et al.[6] (see Table 1).

Model II. To compare the simple three-site model to a hopefully more realistic model for *tert*-butyl alcohol, we have also constructed a fully flexible all-atom model (see Figure 1). Again, the geometry and the atomic charges are taken from the work by Noto et al.[6] Potential parameters are given in Table 3. In addition, the O−H stretching is made anharmonic by means of a Morse type potential, previously shown to describe hydrogen bonded O−H···O systems well.[21,22] The bonded potential parameters are based on our previous flexible all-atom methanol model,[22] with the addition of new bonded parameters. All parameters for the bonded interactions are given in Table 4.

Simulation Details. Cubic periodic boundary conditions with the minimum image convention were invoked in all our simulations. The solute−solvent cross-interactions are calculated using the simple Lorens−Berthelot combination rules,[23] and the Coulombic interactions were treated using the Ewald method.[23] Some simulation characteristics and the temperature and the density used in our simulations are given in Tables 5 along with some basic results.

The simulations were carried out on a Fujitsu VX vector parallel supercomputer at the Center for Parallel Computers at the Royal Institute of Technology (KTH) in Stockholm and on the departmental parallel Beowulf Linux PC cluster[24] at the division of Physical Chemistry, Stockholm University.

Rigid Model, Model I. In the case of the rigid molecular model I, we simply diagonalize the moment of inertia tensor to determine the molecular coordinate system. The principal Z-axis of TBA lies approximately along its oxygen-trimethyl bond (see Figure 1). The translational equations of motion for the molecular centers-of-mass are solved using the Verlet Leapfrog algorithm. The quaternion-based Leapfrog algorithm by Fincham[25] was used to numerically solve the Eulerian equations for the angular motion of the molecules, with a time step of 1.0 fs. The simulations are carried out in the NVT ensemble using a Nóse−Hoover[26] thermostat with a relaxation time of 30 fs. The simulation software is a modified version of McMoldyn.[27]

TABLE 4: Bonded Potential Parameters for the 15-site Model (model II) of *tert*-Butyl Alcohol

	bonded interactions		
bond	K_B (kJ/mol/Å)	R_{eq} (Å)	comment
O−H	2284	0.9292	Morse potential[a]
$O-C_{tb}$	1580	1.4164	
$C_{tb}-C_m$	923	1.5240	
C_m-H_m	1294	1.111	

angle	K_Φ (kJ/mol/deg)	Φ_{eq} (deg)
$H-O-C_{tb}$	195.4	111.28
$O-C_{tb}-C_m$	314.0	111.28
$C_m-C_{tb}-C_m$	222.3	108.745
$C_{tb}-C_m-H_m$	143.1	111.445
$H_m-C_m-H_m$	147.3	108.754

dihedral angle	phase angle (degr)	K_{DIH} (kJ/mol)	multiplicity
$H-O-C_{tb}-C_m$	0.0	0.58	3
$O-C_{tb}-C_m-H_m$	0.0	0.83	3
$C_m-C_{tb}-C_m-H_m$	0.0	0.83	3

[a] $D = 376.35$ kJ/mol. $\rho = 2.440$ Å^{-1}.

TABLE 5: Some Characteristic Parameters and Results from the Simulations of the Pure Liquid of TBA

quantity	model I	model II
no. of $(CH_3)_3COH$ molecules	256	128
temperature (K)	300	300
ρ(g/cm^3)	0.75	0.7856
cutoff (Å)	10.0	10.0
$\langle U_{TOT}\rangle$	-29.7 ± 0.8	-447.4 ± 0.04
$\langle U_{INTER}\rangle$	-29.7 ± 0.8	-26.9 ± 0.2
D_v ($\times 10^{-9}$ m^2/s)	3.03	1.31 (exptl: 0.33[b])
simulation (ns)	0.4	0.6

[a] All energies are in kJ/mol. Note that for model II there is a large intramolecular contribution to the potential energies from the electrostatic 1−4 interactions. [b] At 301 K, Kipkemboi, Easteal *Bull. Chem. Soc. Jpn.* **1994**, *67*, 2956−2961.

Flexible Model, Model II. For our flexible molecules, the Newtonian equations were solved for each atom allowing for all possible molecular translations and rotations. All simulations are carried out in the NPT ensemble. The temperature and pressure are maintained by a Nóse−Hoover thermostat[26] and barostat, with corresponding coupling parameters of 30 and 700 fs respectively. The method of multiple time steps by Tuckerman et al.[28] was used in the simulations. Rapidly fluctuating forces from the stretching of the covalent bonds and angles, as well as the nearest-neighbor nonbonded interactions were calculated every 0.2 fs, while a time step of 2.0 fs was used for other, slower fluctuating interactions. The software used was the parallel scalable general purpose simulation package *M.Dyna-Mix*.[29] The method of accumulation and visualization of the spatial distribution function (SDF) data is discussed in ref 2.

Results and Discussion

We have compared the two TBA potential models in simulations of the pure liquid alcohol. We recall that *tert*-butyl alcohol freezes at 25.66 °C so our simulations of TBA(l) were carried out slightly above the freezing point at 300 K. Other simulation details for pure liquid TBA are given in Table 5. Note that the total potential energy from the two models differ substantially because of the intramolecular energies, coming from bond stretching, angle bending, and motion of the torsional

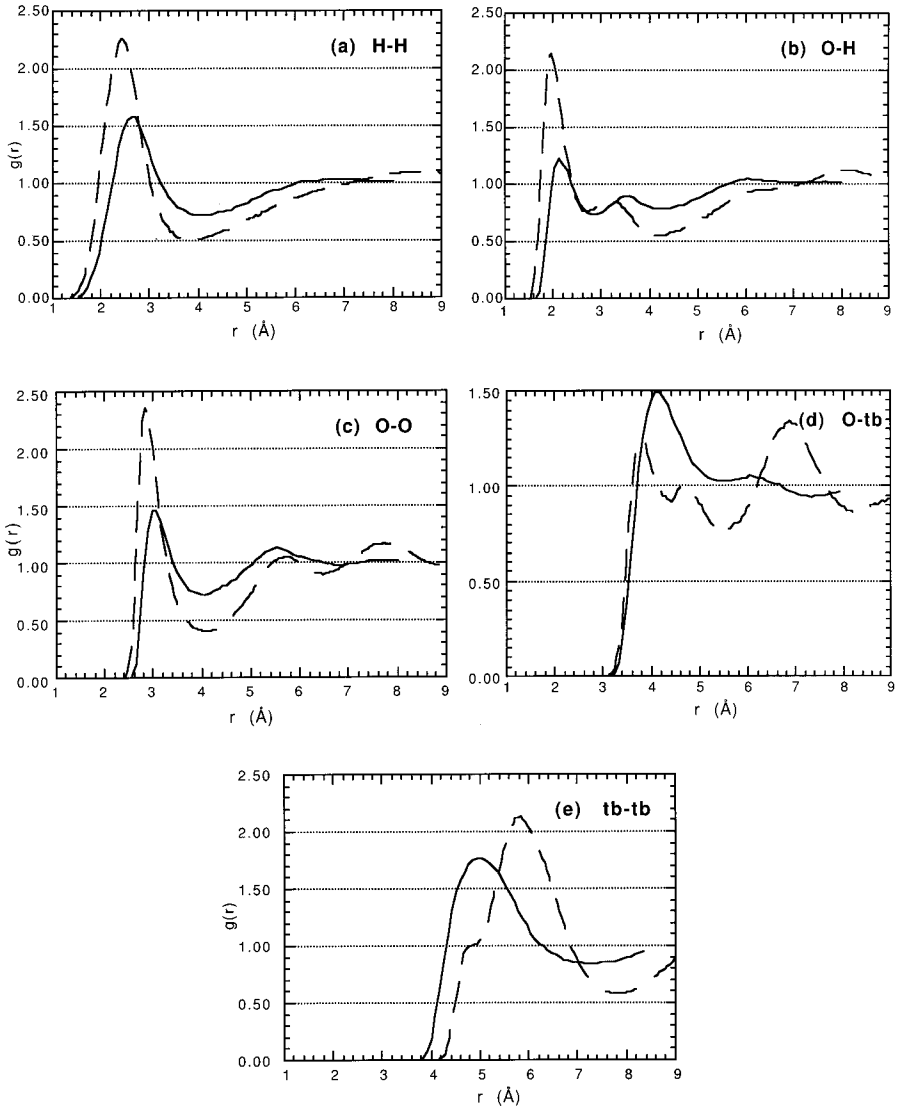

Figure 2. Radial distribution functions, $g(r)$, for pure liquid TBA at 300 K. The solid lines are results for model I, while dashed lines were obtained with model II. (a) Hydroxyl hydrogen−hydroxyl hydrogen. (b) Oxygen−hydroxyl hydrogen. (c) Oxygen−oxygen. (d) Oxygen−*tert*-butyl (tb). (e) tb−tb.

angles (internal rotations in the case of TBA), have been included in model II. Also included are the so-called 1−4 interactions, i.e., internal nonbonded interactions beyond three bonds, where the dominant contribution to the 1−4 energy is due to the Coulombic interactions. We can see from Table 5 that model I substantially overestimates the self-diffusion coefficient, D, for TBA. Model II improves on this estimate, but is still more than a factor of 4 too high. This is our first indication that both models appear to underestimate the degree of H-bonding in the liquid, and model I more so than model II. This will be confirmed by our structural analysis below.

Our analysis of the liquid structure of *tert*-butyl alcohol will utilize both radial distribution functions (RDFs) between atoms or sites, as well as the so called spatial distribution functions (SDFs). It has been previously shown[2] that these spatially resolved (three-dimensional) functions provide a much more complete description of the structure in molecular liquids.

The RDFs between corresponding sites or groups are compared in Figure 2 for model I and model II. Figure 3 shows two additional results for model II, in particular the RDFs between the central carbon and the methyl carbons, and the oxygen and the methyl carbons. The peak positions of first maxima are given with the corresponding intensities in Table 6

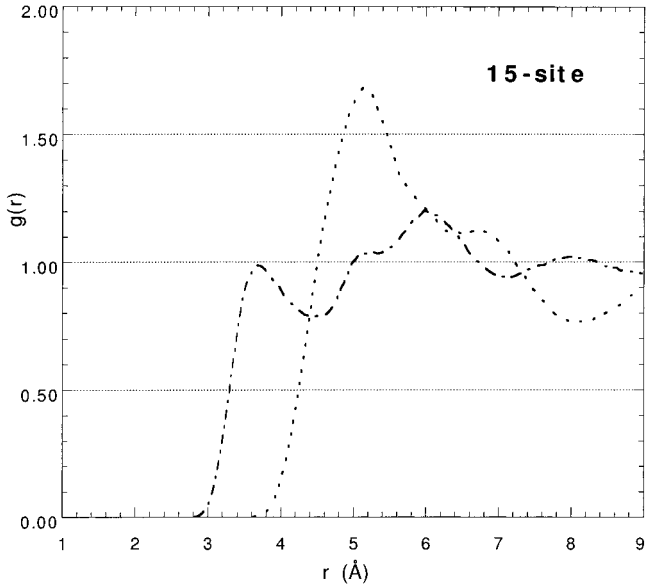

Figure 3. Radial distribution functions, $g(r)$, for model II in pure liquid TBA at 300 K. Dotted line: central (tb) carbon−methyl carbon. Dashed−dot line: oxygen−methyl carbon.

TABLE 6: Approximate Peak Positions and Intensities (*I*) of the Radial Distribution Functions between the Hydroxyl Groups of *tert*-Butyl Alcohol

peak[a]	model I[b]	model II[b]	Yonker et al.[7]	Bowron et al.[9]
M(O−O)	2.98	2.83		2.8
I(O−O)	1.5	2.35		8.5
m(O−O)	4.00 (1.17)	4.1 (1.32)		3.4
M(O−H)	2.21	1.97	−1.9	1.9
I(O−H)	1.25	2.15	−11	9
m(O−H)	2.89 (1.62)	2.72 (1.77)	−2.5	2.5
M(H−H)	2.70	2.43		2.4
I(H−H)	1.58	2.27		6.9

[a] *M* is the first maximum and *m* is the first minimum, in angstroms. [b] The numbers quoted in parentheses are the corresponding coordination numbers calculated by integrating to the first minimum.

along with the positions of their first minima and coordination numbers. Also included in Table 6 are the corresponding values available from other studies. We can see from Figure 2 that the simple three-site model (model I) and the all-atom 15-site model (model II) give qualitatively similar results for the direct hydrogen bonding between the TBA molecules. The positions of the first maxima for model I are, however, shifted consistently to larger distances for all three pairs OO, OH, and HH by 0.15, 0.24, and 0.27 Å, respectively, and the peaks are broader when compared to model II; the values for model II are in better agreement with the results obtained using the OPLS model (see Table 6). The fact that the peaks for the OO and OH $g(r)$ are broader and less well defined suggests that H-bonding is not as strong on average in model I (even though it uses essentially the same site charges as model II). Explicit comparison with OO, OH, and HH functions with those of Bowron et al.[9] indicates that even the results for model II are considerably less structured than those from the OPLS model. Moreover, the split peak features observed in the modified potential model RDFs of ref 9, which would suggest two distinct types of near-neighbors, are not evident. The main difference between the present results and those obtained with the OPLS model would seem to be the apparent strength of hydrogen bonds. Since normal hydrogen bonds are mainly electrostatic interactions, the primary reason for the difference can be found in the disparity of the atomic charges assigned to the hydroxyl oxygen and hydrogen in the OPLS model and in our models (see Table 1). In the OPLS model the charges have been deliberately set to give roughly a 25% larger dipole moment for the molecule compared to its gas-phase value. One of the conclusions of Bowron et al.[9] was that the unmodified OPLS potential appears to overemphasize H-bonding. We have chosen to use the smaller charges obtained by Noto et al.[6] in their calculations at the 6-31G(d,p) level, where they obtained a very good agreement with the experimental (gas phase) dipole moment for $(CH_3)_3C-NO$, the other molecule they had studied.

In Figure 2 the RDF involving the center-of-mass (COM) points of the *tert*-butyl (tb) groups for model I and the corresponding curves between the central (tb) carbons for model II are also shown. It should be emphasized that these two points do not coincide to the same point in the molecule. The distance from the hydroxyl oxygen to the *tert*-butyl COM is 1.836 Å while the distance from the hydroxyl oxygen to the *tert*-butyl central carbon is only 1.4164 Å. The difference in the molecular geometries can be seen in Figure 2e. We can see that in constructing model I we were forced to compromise because any further increase in the size of the Lennard-Jones sphere for the *tert*-butyl group would have led to a situation where the hydroxyl group would be found effectively inside the bulky alkyl group. Additionally, model I seems to miss completely the shoulder on the first peak between the tb groups. This shoulder is visible in the work of Bowron et al.[9] in their neutron diffraction study of the structure of the liquid TBA using empirical potential function refinement. However, in their Monte Carlo simulations using the OPLS parameter set this shoulder grows to become the major peak while the main peak reduces considerably its intensity. This would suggest that this system is over structured presumably because the atomic charges used in the OPLS model are too large. The oxygen−tb RDF shown in Figure 2d also exhibits considerable difference between the two models. While showing roughly the same distance of closest approach of these two sites, the $g(r)$ for models I and II then generally differ in the positions and amplitudes of their subsequent peaks. This suggests that the apparent balance between hydrophobic and hydrophilic forces is different in the two models. We point out that the O−tb RDF for model II is similar to the results of Bowron et al.[9]

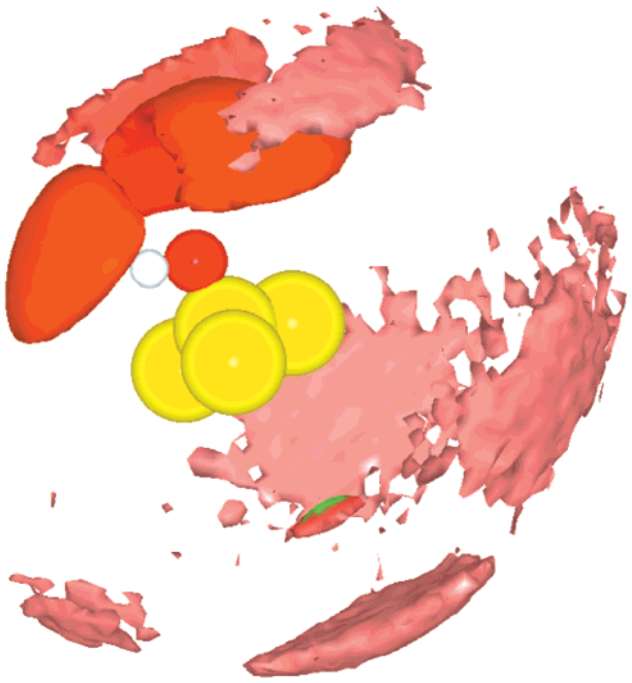

Figure 4. Oxygen−oxygen spatial distribution function for model II at a threshold of 1.7. The surfaces are shaded by separation distance, darker corresponding to smaller separations.

In Figure 3 two additional RDFs for model II are shown. We note that these functions are not defined for the three-site model I. Comparing the central (tb) carbon−oxygen and oxygen−methyl carbon RDF functions to the comparable functions of the empirical potential structure refinement study of Bowron et al.,[9] we again find basic agreement. Generally, we find that the present results for model II exhibit somewhat less structure.

To get more direct detailed insights into the three-dimensional local structure around TBA, spatial distribution functions[30] were calculated. In Figure 4, the oxygen−oxygen SDF for model II is shown for a threshold of 1.7 times the bulk density, where features have been shaded according to their separation. The two darkest features in Figure 4 are due to hydrogen-bonded nearest neighbors. Both of these features appear considerably distorted, indicating that packing and steric effects are important in influencing the arrangements of these nearest neighbors. We can see that the acceptor is somewhat skewed forward in front of the hydrogen, while donor has become rather broad and skewed backward. Secondary H-bond neighbor features also become evident above the OH group. When the isosurface

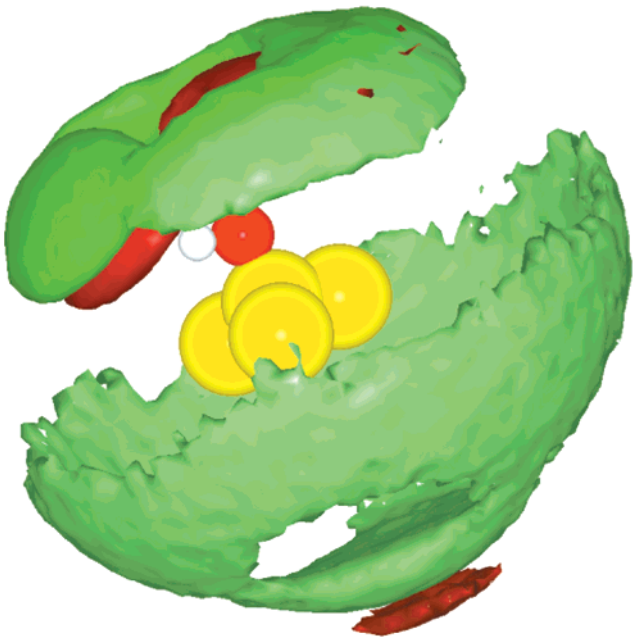

Figure 5. Oxygen−carbon spatial distribution function (green) for model II at a threshold of 2.3, overlayed with the oxygen−oxygen SDF (red) with a 2.0 threshold. The surfaces are shaded by separation, darker corresponding to smaller values.

threshold is lowered slightly, these features quickly grow to form a half-ring around the back half of the OH group. Upon further reduction of the threshold this secondary structure will eventually connect to the bowl that will grow in below the molecule. Below the OH group of TBA, the most intense peaks from neighboring oxygens are due to preferred *tert*-butyl group hydrophobic associations. As the threshold is lowered further, the entire lower bowl quickly grows in to enclose the molecule.

In Figure 5, the *tert*-butyl group central-carbon SDF is shown at an isosurface threshold of 2.3 for model II, overlayed with neighboring oxygen densities for a 2.0 threshold. The large feature below the $C(CH_3)_3$ group represents the hydrophobic association of *tert*-butyl groups and we can again observe that there are slightly more preferred positions. We note that the small (red) feature below the large (green) cap is due to local oxygen density. If the threshold is decreased further the (green) bowl, representing carbon density, will quickly surround the whole molecule. Above the molecule (and appearing darkest) are the expected oxygen density features due to H-bond neighbors. The ring of carbon density (which will join the bowl from below upon reduction of the threshold) is partially associated with the nearest H-bonded neighbors.

The spatial distributions functions for model I (not shown) show similar general features to those for model II. They differ in a couple of important, yet expected, respects. No specific preference for hydrophobic association is observed around the *tert*-butyl sphere. Hydrogen-bonding features also appear less well resolved, consistent with weaker H-bonding in this liquid. Particularly, the feature due to neighboring oxygen density associated with H-bond accepting neighbors becomes even more distorted than we find in Figure 4 for model II. For model I, this feature stretches forward and down to become almost continuously connected to the cap of neighbor density due to hydrophobically associated neighbors. Thus, it becomes clear from this SDF that the weak H-bonding in model I is due to the steric bulk of the Lennard-Jones sphere representing the *tert*-butyl group which hinders the close approach of neighboring oxygen atoms.

Conclusions

In this paper we have reported computer simulation results exploring in detail the local structure in liquid *tert*-butyl alcohol (TBA). Molecular dynamics simulations were carried out for a simple rigid three-site model and a flexible all-atom 15-site potential. Model systems of the pure liquid of TBA were studied at 300 K. Radial distributions functions (RDF) were employed to aid in our structural analysis, however spatial distribution functions (SDF), correlation functions that span the full three-dimension space surrounding a molecule, were used to provide more detailed information about the local environments in these liquid systems. As in previous work, it was found that the SDFs provide a much more complete and unambiguous picture of the local liquid structure.

Generally, we find that the simple three-site model has some weaknesses in describing the pure liquid where some experimental results are available (as derived from structure factors from neutron scattering). The 15-site model appears clearly superior, being better able to represent pure liquid TBA. While the three-site model is successful at reproducing effects due to the presence of a large hydrophobic group, it only appears to be able to reproduce the behavior of TBA at this qualitative level. From comparisons with previous work, we have noted a sensitivity to the magnitude of the site charges used, and hence the strength of the H-bonding. In the pure liquid we observe that each TBA molecule makes roughly two H-bonds to neighboring molecules. Yet, from distortion of these H-bond features in the SDF, we can also conclude that the TBA molecules are somewhat frustrated by packing and steric effects in making these bonds. As a result, the liquid-state structure is quite sensitive to how the chosen model balances these competing forces. An association of the *tert*-butyl groups can also be seen in the pure liquid, where for the 15-site model some preferential arrangements become evident. No clear indication of appreciable chain formation was observed with either model studied.

In the following paper we will use the same detailed structural approach to examine the structure of the same two TBA models in aqueous solution.[31]

Acknowledgment. This work has been supported by the Swedish Natural Science Research Council (NFR) and by the Natural Science and Engineering Research Council of Canada (NSERC).

References and Notes

(1) Reichardt, C. *Solvents and Solvent Effects in Organic Chemistry;* VCH: Weinheim, 1988.

(2) Kusalik, P. G.; Laaksonen, A.; Svishchev, I. M. Spatial Structure in Molecular Liquids. In *Theoretical and Computational Chemistry Series*; Elsevier: Amsterdam, 1999.

(3) Odelius, M.; Laaksonen, A. Combined MD simulation−NMR Relaxation Studies of Molecular Motion and Intermolecular Interactions. In Theoretical and Computational Chemistry Series; Elsevier: Amsterdam, 1999.

(4) *Handbook of physics and Chemistry*, 66th ed.*;* Chemical Rubber: Boca Raton, FL, 1986.

(5) Kusalik, P.; Lyubartsev, A. P.; Bergman, D. L.; Laaksonen, A. *J. Phys. Chem. A* **2000**. In press.

(6) Noto, R.; Martorana, V.; Emanuele, A.; Fornili, S. L. *J. Chem. Soc., Faraday Trans.* **1995**, *91*, 3803−3808.

(7) Yonker, C.; Wallen, S.; Palmer, B.; Garrett, B. *J. Phys. Chem. A* **1997**, *101*, 9564−9570.

(8) Gao, J. L.; Habibollazadeh, D.; Shao, L. *J. Phys. Chem.* **1995**, *99*, 16460−16467.

(9) Bowron, D. T.; Finney, J. L.; Soper, A. K. *Mol. Phys.* **1998**, *93*, 531−543.

(10) Bowron, D. T.; Finney, J. L.; Soper, A. K. *J. Phys. Chem. B* **1998**, *102*, 3551.

(11) Chen, J.; Bartell, L. *J. Phys. Chem.* **1993**, *97*, 10645−10648.
(12) Hartsough, D.; Merz, K. *J. Phys. Chem.* **1995**, *99*, 384−390.
(13) Ferrario, M.; Klein, M.; McDonald, I. *J. Chem. Phys.* **1987**, *87*, 4823−4828.
(14) Kido, J.; Machida, M.; Kobayashi, T. *J. Kor. Phys. Soc.* **1996**, *29*, S542−S546.
(15) Nakanishi, K.; Ikari, K.; Okazaki, S.; Touhara, H. *J. Chem. Phys.* **1984**, *80*, 1656−1670.
(16) Matsuoka, O.; Clementi, E.; Yoshimine, M. *J. Chem. Phys.* **1976**, *64*, 1351.
(17) Tanaka, H.; Nakanishi, K.; Touhara, H. *J. Chem. Phys.* **1984**, *81*, 4065−4073.
(18) Jorgensen, W. L.; Madura, J. D.; Swenson, C. J. *J. Am. Chem. Soc.* **1984**, *106*, 6638−6646.
(19) Jorgensen, W. L. *J. Phys. Chem.* **1986**, *90*, 1276−1284.
(20) Haughney, M.; Ferrario, M.; McDonald, I. R. *Mol. Phys.* **1986**, *58*, 849−853.
(21) Toukan, K.; Rahman, A. *Phys. Rev. B* **1985**, *31*, 2643.
(22) Wang, J.; Boyd, R. J.; Laaksonen, A. *J. Chem. Phys.* **1996**, *104*, 7261−7269.
(23) Allen, M. P.; Tildesley, D. J. *Computer Simulations of Liquids;* Oxford Science: Oxford, 1985.
(24) For a Hälge−A Linux cluster, see*:* http://www.fos.su.se/physical/aatto/helge/.
(25) Fincham, D. Information quarterly, ccp5 (2) Technical report. September**,** 1981.
(26) Nosé, S. *Mol. Phys.* **1984**, *52*, 255.
(27) Laaksonen, A. *Comput. Phys. Commun.* **1986**, *42*, 271−300.
(28) Tuckerman, M.; Berne, B.; Martyna, G. *J. Chem. Phys.* **1992**, *97*, 1990.
(29) Lyubartsev, A. P.; Laaksonen, A. *Comp. Phys. Commun.* **2000**, *128*, 565−589.
(30) Svishchev, I. M.; Kusalik, P. G. *J. Chem. Phys.* **1993**, *99*, 3049.
(31) Kusalik, P. G.; Lyubartsev. A. P.; Bergman, D. L.; Laaksonen, A. *J. Phys. Chem. B* **2000** *104*, 9533.